A Comparison between the TORUS and AFIR Axial-Flux Permanent-Magnet Machine Using Finite Element Analysis

Amin Mahmoudi
Faculty of Engineering
University of Malaya
50603 Kuala Lumpur, Malaysia
mahmoudi@siswa.um.edu.my

Hew Wooi Ping
Faculty of Engineering
University of Malaya
50603 Kuala Lumpur, Malaysia
nasrudin@um.edu.my

Nasrudin Abdul Rahim
Faculty of Engineering
University of Malaya
50603 Kuala Lumpur, Malaysia
wphew@um.edu.my

***Abstract*— This paper presents a comparison between TORUS and AFIR, the two topologies for double-sided axial-flux permanent-magnet machines. Their slotted and non-slotted topologies were investigated and compared in terms of power density and torque quality. The critical field analysis of the topologies was by finite element method. Results show TORUS topology's high power-density in high current-density and low electrical-loading. AFIR topology has high power in low current-density and high electrical-loading. Non-slotted TORUS and AFIR AFPM machines have negligible cogging torque and lower ripple torque than their slotted counterparts.**

Keywords- axial-flux; permanent-magnet; slotted; slotless; wind generator

I. INTRODUCTION

Axial-flux permanent-magnet (AFPM) machine is an attractive alternative to radial-flux permanent-magnet (RFPM) machine. Axial-flux permanent-magnet (AFPM) machine's high efficiency and torque-to-weight ratio spur research into various applications [1]. In conventional machines, air-gap flux density usually is radial; in AFPMs, it is mainly axial. AFPMs generally exhibit an axial length much shorter than that of a conventional motor of the same rating, so, choosing an AFPM machine of compatible construction and characteristic is the most important issue in literatures.

Double-sided axial-flux permanent-magnet (AFPM) motors are the most promising and widely-used types. Two topologies for double-sided AFPM machines are slotted axial-flux one-stator-two-rotor (TORUS) and two-stator-one-rotor (AFIR) [2]. Their characteristic is an important parameter, especially in wind generator applications. Comparison between slotted and non-slotted types of the two double-sided AFPM topologies in terms of torque density, torque quality, and compatibility with wind generator seems necessary. Presented here is an appropriate selection of AFPM for wind generator. Figs. 1 and 2 show single-stator double-rotor (TORUS) and double-stator single-rotor (AFAIR) as different constructions of double-sided AFPM machines, selected for study [3].

Maximum torque density in AFPM motors changes with increased air-gap length; different topologies, different changes. Minimization of cogging and ripple torque including modifying the winding structure and skewing the rotor magnets differs in various structures. To evaluate the characteristics of various AFPM machines, their magnetic field is computed via Finite Element Method (FEM), which is more accurate than the other methods are [4].

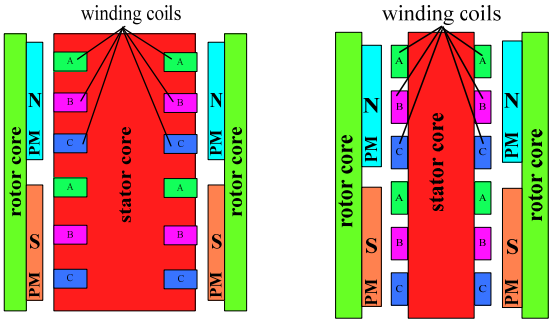

(b) slotted stator TORUS AFPM machine (c) slotless stator TORUS AFPM machine

Fig. 1. Single-stator double-rotor AFPM machine (TORUS)

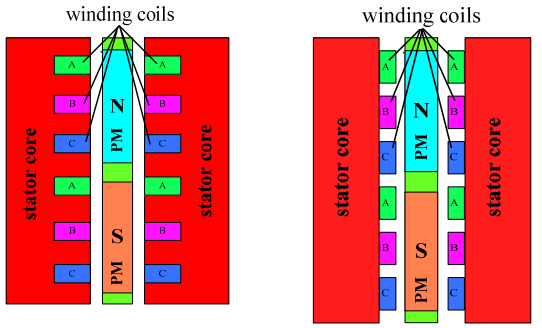

(b) slotted stator AFIR permanent-magnet machine (c) slotless stator AFIR permanent-magnet machine

Fig. 2. Double-stator single-rotor AFPM machine

II. METHODOLOGY

Comparing of machine types is generally a formidable task, as variables exist for each machine, making those variables to be held constant for comparison difficult to select. One method of comparing is the sizing equation, which is based on air-gap

surface diameter and effective stack length [5]. Assuming negligible leakage inductance and resistance, rated power is:

$$P_{out} = \eta \frac{m}{T}\int_0^T e(t)\cdot i(t)\,dt = mK_p \eta E_{pk} I_{pk} \qquad (1)$$

$e(t)$ is phase air-gap EMF, $i(t)$ is phase current, η is machine efficiency, m is number of machine phases, and T is period of one EMF cycle. E_{pk} and I_{pk} are peaks of phase air-gap EMF and of current, respectively. K_p is electrical power waveform factor, defined as:

$$K_p = \frac{1}{T}\int_0^T \frac{e(t)\cdot i(t)}{E_{pk}\cdot I_{pk}}dt = \frac{1}{T}\int_0^T f_e(t)\cdot f_i(t)dt \qquad (2)$$

where $f_e(t)=e(t)/E_{pk}$ and $f_i(t)=i(t)/I_{pk}$ are expressions for normalized EMF and current waveforms. For effect of current waveform, current waveform factor (K_i) is defined:

$$K_i = \frac{I_{pk}}{I_{rms}} = \frac{1}{\sqrt{\frac{1}{T}\int_0^T \left(\frac{i(t)}{I_{pk}}\right)^2 dt}} \qquad (3)$$

where, I_{rms} is phase-current rms value. Table I lists typical waveforms and their corresponding power-waveform factor (K_p) and current-waveform factor (K_i) [5]. Peak value of phase-air-gap EMF for equation (8)'s AFPM motor is:

$$E_{pk} = K_e N_{ph} B_g \frac{f}{p}(1-\lambda^2)D_o^2 \qquad (4)$$

K_e is EMF factor incorporating winding distribution factor (K_w) and per-unit portion of air-gap area-total spanned by machine's salient poles (if any); N_{ph} is number of turns per phase; B_g is flux density in air gap; f is converter frequency; P is machine pole pairs; λ is AFPM diameter ratio D_i/D_o; D_o is diameter of machine outer surface; D_i is diameter of machine inner surface. Equation (9)'s peak phase current is:

$$I_{pk} = A\pi K_i \frac{1+\lambda}{2}\frac{D_o}{2m_1 N_{ph}} \qquad (5)$$

where, m_1 is number of phases of each stator, and A is electrical loading. Other authors have provided a general-purpose sizing equation for AFPM machines; it takes the following form:

$$P_{out} = \frac{1}{1+K_\phi}\frac{m}{m_1}\frac{\pi}{2}K_e K_i K_p K_L \eta B_g A \frac{f}{P}(1-\lambda^2)\frac{1+\lambda}{2}D_o^2 L_e \qquad (6)$$

m_1 is number of phases of each stator; L_e is effective axial length of the motor; K_φ is electrical loading ratio on rotor and stator; K_L is aspect ratio coefficient pertinent to a specific machine structure, with considerations for effects of losses, temperature rise, and the design's efficiency requirements. Also, machine torque density for volume total is defined as:

$$\tau_{den} = \frac{P_{out}}{\omega_m \frac{\pi}{4} D_{tot}^2 L_{tot}} \qquad (7)$$

ω_m is rotor angular speed, D_{tot} and L_{tot} respectively are machine-outer-diameter total and machine-length total including stack-outer-diameter and end-winding-protrusion from radial and axial iron stacks.

TABLE I
Typical prototype waveforms

Model	e(t)	i(t)	K_i	K_p
Sinusoidal	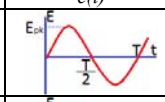	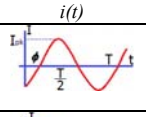	$\sqrt{2}$	0.5Cosφ
Sinusoidal	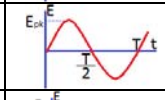	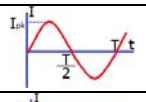	$\sqrt{2}$	0.5
Rectangular		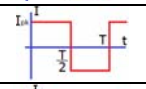	1	1
Trapezoidal	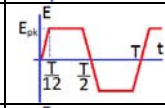	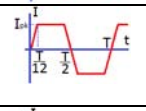	1.134	0.777
Triangular	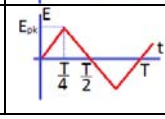	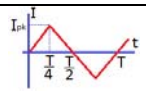	$\sqrt{3}$	0.333

Machine outer-diameter total D for the AFPM machines is:

$$D_{tot} = D_o + 2W_{cu} \qquad (8)$$

where W_{cu} is protrusion of end winding from iron stack, in radial direction. For back-to-back wrapped winding, protrusions exist towards machine axis as well as towards the outsides, and can be calculated as:

$$W_{cu} = \frac{D_i - \sqrt{D_i^2 - \frac{2AD_{ave}}{\alpha_s K_{cu} J_s}}}{2} \qquad (9)$$

where, D_{ave} is average diameter of the machine, J_s is current density, and K_{cu} is copper fill factor. α_s is the ratio of stator teeth portion to the stator pole pitch portion and for the non-slotted topology machines is α_s =1.

The axial length of the machine is:

$$L_e = \begin{cases} L_s + 2L_r + 2g & for\ TORUS \\ 2L_s + L_r + 2g & for\ AFIR \end{cases} \qquad (10)$$

L_r is axial length of rotor, and g is air-gap length. Axial length of stator L_s can be written as:

$$L_s = \begin{cases} L_{cs} + 2L_{ss} & for\ TORUS \\ L_{cs} + L_{ss} & for\ AFIR \end{cases} \qquad (11)$$

Axial length of stator core L_{cs} can be written as:

$$L_{cs} = \frac{B_g \pi \alpha_p D_o (1+\lambda)}{4pB_{cs}} \qquad (12)$$

where B_{cs} is flux density in stator core, and α_p is ratio of average air-gap flux density to peak air-gap flux density. Note that for slotted machines, depth of stator slot is $L_{ss}=W_{cu}$.

Axial length of rotor L_r becomes

$$L_r = L_{cr} + L_{pm} \qquad (13)$$

L_{pm} is permanent-magnet length; axial length of rotor core L_{cr} is:

$$L_{cr} = \frac{B_u \pi D_o (1+\lambda)}{8 p B_{cr}} \qquad (14)$$

where B_{cr} is flux density in rotor disc core, and B_u is attainable flux density on permanent-magnet surface. Permanent-magnet length L_{pm} can be calculated as:

$$L_{pm} = \begin{cases} \dfrac{\mu_r B_g}{B_r - \left(\dfrac{K_f}{K_d} B_g\right)} (g + W_{cu}) & for \\ \dfrac{\mu_r B_g}{B_r - \left(\dfrac{K_f}{K_d} B_g\right)} K_c g & for \end{cases} \qquad (15)$$

where μ_r is magnet's recoil relative permeability, Br is permanent-magnet material residual-flux density, K_d is leakage flux factor, K_c is Carter factor, $K_f = B_{gpk}/B_g$ is peak-value corrected factor of air-gap flux density in radial direction of AFPM motor. These factors can be obtained from FEM analysis.

In AFPM motors, air-gap flux density and diameter ratio are two important design parameters significantly affecting motor characteristics. For optimized machine performance, diameter ratio and air-gap flux density must be chosen carefully. The optimum design should maximize power density while maintaining desired efficiency within design restrictions. In design studies, diameter ratio and air-gap flux density are design parameters. Fig. 3 compares various volumes of AFPM machine in five powers. There seems to be no significant difference between volume of optimized slotted and non-slotted TORUS and AFIR machines at low-range powers. Even volume difference between TORUS and AFAIR in the 1kw power range is negligible. As power increases, though, the distinction becomes more obvious. Volume difference in 20 kW can be distinguished for all AFPM introduced machines.

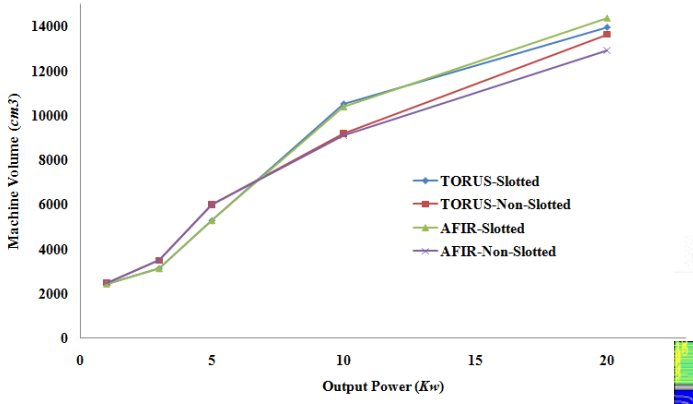

Fig. 3. Volume comparison in five powers

III. Finite Element Analysis

This paper compares torque density of two double-sided AFPM machines in the 10*Kw*-output-power range. Tables II and III respectively list specifications of the slotted and non-slotted TORUS test machines [4].

TABLE II
Dimensions and specifications of the slotted TORUS test machine

Parameter	Symbol	Values
Outer Diameter	D_1	0.3650 m
Inner Diameter	D_2	0.1030 m
Number of pole pairs	P	2
Number of slots	s	12
Magnet-pole arc	α_m	67.0 °
Air-gap length	g	0.0010 m
Slot fill factor	k_f	0.8
Stator-yoke thickness	h_{ys}	0.0420 m
Slot depth	h_t	0.0100 m
Rotor-yoke thickness	h_{yr}	0.0250 m
Magnet's axial length	L_m	0.0020 m

TABLE III
Dimensions and specifications of the non-slotted TORUS test machine

Parameter	Symbol	Values
Outer Diameter	D_1	0.4819 m
Inner Diameter	D_2	0.1234 m
Number of pole pairs	P	2
Number of slots	s	0
Magnet-pole arc	α_m	67.0 °
Air-gap length	g	0.0010 m
Slot fill factor	k_f	0.8
Stator-yoke thickness	h_{ys}	0.0286 m
Slot depth	h_t	0 m
Rotor-yoke thickness	h_{yr}	0.0110 m
Magnet's axial length	L_m	0.0018 m

Figs. 4 and 5 respectively show the magnetic flux density and the flux distribution over one pole pair, of slotted-TORUS topology at full-load conditions.

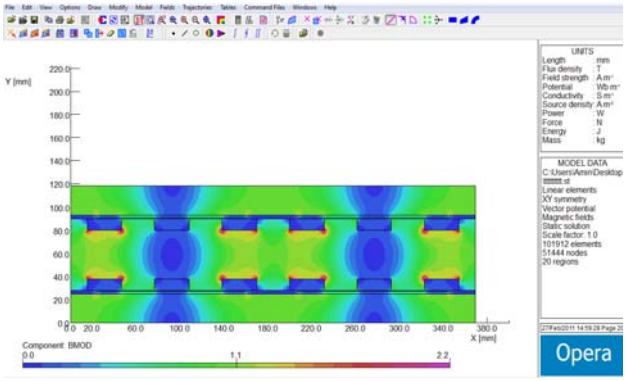

Fig. 4. Magnetic flux density distribution for slotted-TORUS topology

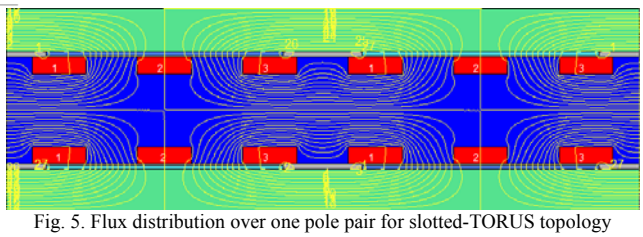

Fig. 5. Flux distribution over one pole pair for slotted-TORUS topology

Figs. 6 and 7 respectively also show the magnetic flux density and the flux distribution over one pole pair, of non-slotted-TORUS topology at full-load conditions.

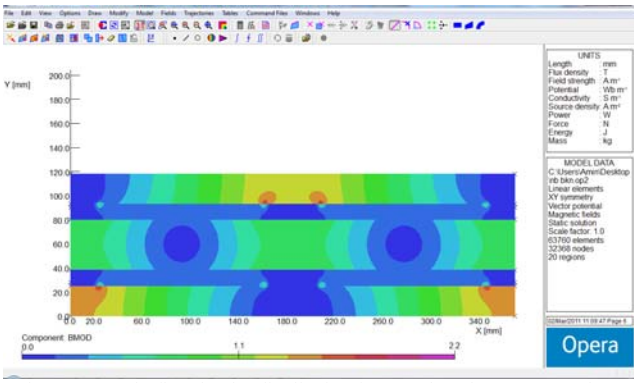

Fig. 6. Magnetic-flux-density distribution for non-slotted-TORUS topology

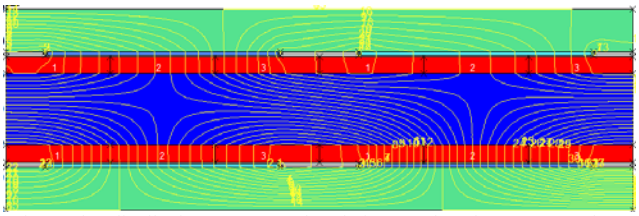

Fig. 7: Flux distribution over one pole pair for non-slotted-TORUS topology

Tables IV and V respectively list specifications of the slotted and the non-slotted AFIR test machines [4].

TABLE IV
Dimensions and specifications of the slotted AFIR test machine

Parameter	Symbol	Values
Outer Diameter	D_1	0.3650 m
Inner Diameter	D_2	0.1030 m
Number of pole pairs	P	2
Number of slots	s	12
Magnet-pole arc	α_m	67.0 °
Air-gap length	g	0.0010 m
Slot fill factor	k_f	0.8
Stator-yoke thickness	h_{ys}	0.0420 m
Slot depth	h_t	0.0100 m
Rotor-yoke thickness	h_{yr}	0.0250 m
Magnet's axial length	L_m	0.0020 m

TABLE V
Dimensions and specifications of the non-slotted-AFIR test machine

Parameter	Symbol	Values
Outer Diameter	D_1	0.4540 m
Inner Diameter	D_2	0.1250 m
Number of pole pairs	P	2
Number of slots	s	12
Magnet-pole arc	α_m	67.0 °
Air-gap length	g	0.0010 m
Slot fill factor	k_f	0.8
Stator-yoke thickness	h_{ys}	0.0107 m
Slot depth	h_t	0.0090 m
Rotor-yoke thickness	h_{yr}	0.0400 m
Magnet's axial length	L_m	0.0022 m

Fig. 8 shows air-gap-flux density at no-load conditions versus electrical angle for both slotted and non-slotted TORUS topologies. Sudden change in air-gap magnetic reluctance owing to existence of slots in slotted TORUS machine causes oscillation in air-gap flux density. In non-slotted TORUS machine, flux density at the edges of the permanent-magnet is higher than its values at the center of the permanent magnet.

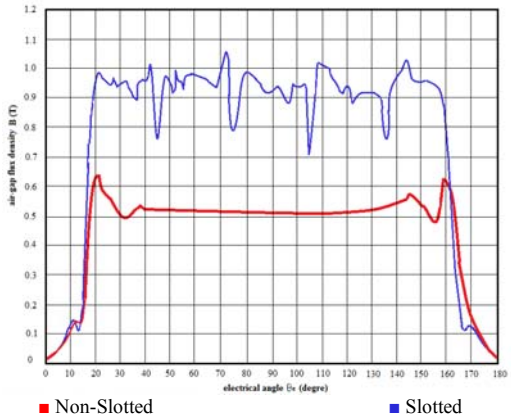

Fig. 8: Air-gap-flux density at no-load conditions versus electrical angles, TORUS topology

Figs. 9 and 10 respectively show magnetic flux density and flux distribution over one pole pair, for slotted-AFIR topology at full-load conditions.

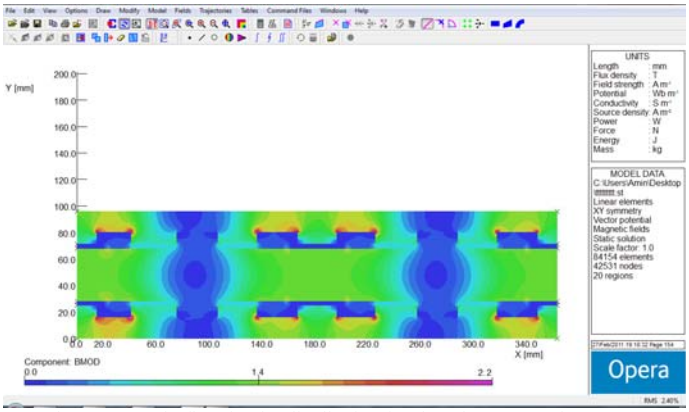

Fig. 9. Magnetic-flux-density distribution for slotted-AFIR topology

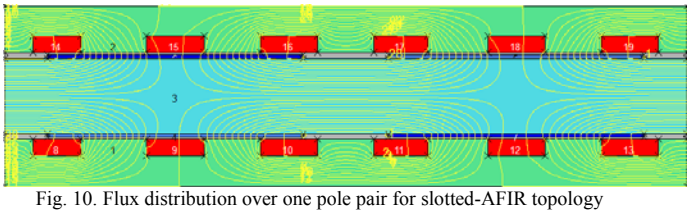

Fig. 10. Flux distribution over one pole pair for slotted-AFIR topology

Figs. 11 and 12 respectively also show the magnetic flux density and the flux distribution over one pole pair, of non-slotted-AFIR topology at full-load conditions.

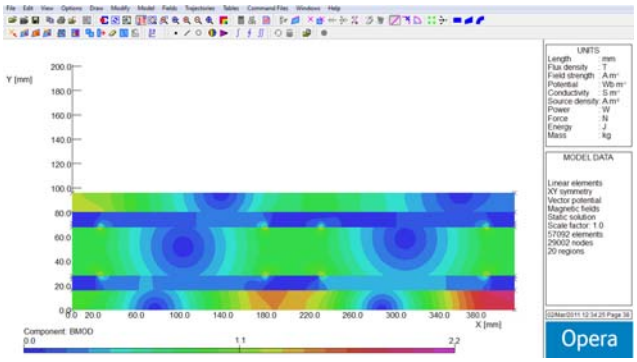

Fig. 11. Magnetic-flux-density distribution for non-slotted-AFIR topology

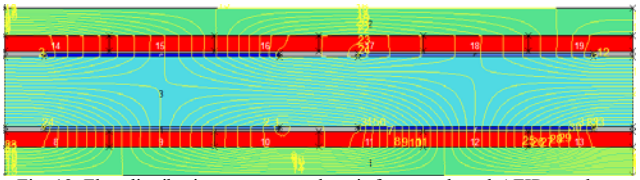

Fig. 12. Flux distribution over one pole pair for non-slotted-AFIR topology

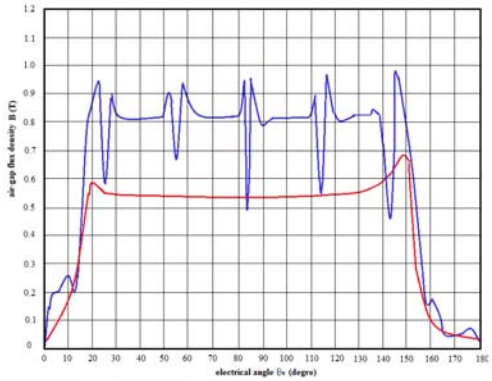

■ Non-Slotted ■ Slotted

Fig. 13. Air-gap flux-density at no-load conditions versus electrical angle, AFIR topology

Fig. 13 shows air-gap flux density at no-load conditions versus electrical angle, for both slotted and non-slotted AFIR topologies. Sudden change in air-gap magnetic reluctance, owing to existence of AFIR slots, causes oscillation in air-gap-flux density. In non-slotted AFIR machine, flux density at the edges of the permanent magnet is higher than at the center of the permanent magnet.

TABLE VI. Cogging torque and ripple torque comparison for various axial-flux permanent-magnet machines, per unit

Parameter	Cogging Torque	Ripple Torque
Slotted-TORUS	0.06	0.15
Non-Slotted-TORUS	0	0
Slotted-AFIR	P	2
Non-Slotted-AFIR	0.06	0.38

The goal here was to find the trend for the total and the cogging torques, versus the electrical angle. Table VI shows per unit, the amount of cogging torque for the AFPM machines presented, whose torque production could thus be compared. Non-slotted AFPM machines in TORUS and AFIR topologies have negligible cogging torque and lower ripple torque than do their slotted counterparts. Their ripple torque is minimized by their magnet-to-pole-arc ratio, their rotor magnets' skew angle, and their winding's distribution shape.

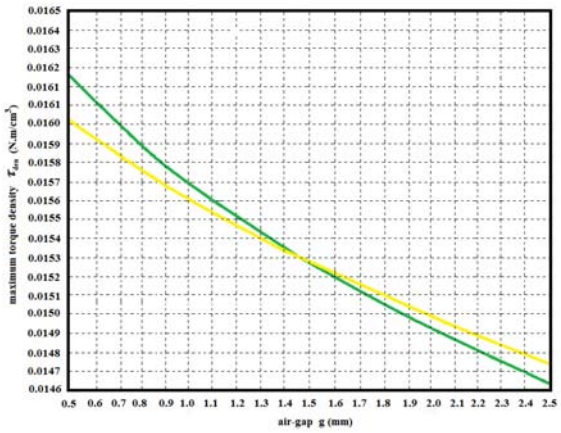

■ TORUS ■ AFIR

Fig. 14. Maximum torque density of TORUS and AFIR versus air-gap flux at A=35000 (A/m)

Fig. 14 shows the maximum torque density of TORUS and AFIR types of AFPM machines versus air-gap flux at A=35000. TORUS topology has high power at high current and low electrical-loading. But, AFIR topology has high power at low current and high electrical-loading. TORUS configuration needs more magnet weight because of additional air-gap owing to stator winding accommodation. Power rating growth results in air-gap increase, which is consequent to larger magnet and winding. For wind-generator applications, TORUS configuration is thus more suitable in low power ratings.

IV. Conclusion

Presented has been a comparison among various double-sided AFPM machine topologies: slotted TORUS, non-slotted TORUS, slotted AFIR, and non-slotted AFIR. For optimum machine design, sizing equations for the topologies were extracted, and their volume compression in five powers were presented. 2D FEA models were developed to yield reasonable predictions for torque quality and for 2D field distribution of both TORUS and AFIR topologies. The non-slotted AFPM machines in both TORUS and AFIR topologies have negligible cogging torque, and lower ripple-torque than do their slotted counterparts. Shown was maximum torque density of slotted TORUS and slotted AFIR machines versus air-gap flux. Results indicate TORUS topology's high power-density in high current-density and low electrical-loading, and AFIR topology's high power in low current and high electrical-loading.

V. REFERENCES

[1] K. Sitapati and R. Krishnan, "Performance comparison of radial and axial field permanent magnet brushless machines", IEEE Transactions on Industry Applications, Vol.37, No.5, Sept/Oct 2001, pp. 1219-1226.

[2] J. F. Gieras, R. J. Wang, and M. J. Kamper, "Axial Flux Permanent Magnet Brushless Machines", (Kluwer Academic Publisher, 2008.

[3] S. A. Gholamian, M. T. Abbasi Ablouie, A. Mohseni and, S. E. Jafarabadi, " Effect of Air Gap on Torque Density for Double-Sided Axial Flux Slotted Permanent Magnet Motors using Analytic and FEM Evaluation, Journal of Applied Sciences Research, Vol. 5, No. 9, 2009, pp. 1230-1238.

[4] A. Mahmoudi, N. A. Rahim, W. P. Hew, "Analytical Method for Determining Axial-Flux Permanent-Magnet Machine Sensitivity to Design Variables" International Review of Electrical Engineering (IREE), Vol. 5, No. 5, September-October 2010, pp. 2039-2048.

[5] S. Huang, J. Luo, F. Leonardi and T. A. Lipo, "A Comparison of Power Density for Axial Flux Machines Based on the General Purpose Sizing Equation", IEEE Trans. on Energy Conversion, Vol.14, No.2, June 1999, pp. 185-192.